第 34 卷第 3 期
2018 年 3 月

无 机 化 学 学 报
CHINESE JOURNAL OF INORGANIC CHEMISTRY

Vol.34 No.3
545-550

4-吡啶-*NH*-1,2,3-三唑构筑的两个 Zn(Ⅱ) 配合物的合成、结构和荧光性质

雷 雪 陈云舟 李元祥 贾丽慧* 陈云峰*
(武汉工程大学化学与环境工程学院,武汉 430073)

摘要：以 4-吡啶-*NH*-1,2,3-三唑(L)为配体与 $ZnCl_2 \cdot H_2O$ 分别在溶剂热和室温挥发条件下得到了配合物$[Zn_2(L)_2Cl_4]$ (**1**)和$[Zn(L)_2Cl_2] \cdot 2H_2O$ (**2**),并进行了红外、元素分析、单晶衍射、粉末衍射等表征。2 个配合物中,超分子相互作用对于配合物的结构有很大影响。其中,配合物 **1** 由氢键和 π-π 相互作用形成 3D 堆积结构,配合物 **2** 通过氢键作用形成堆积结构。同时,在常温下研究了配体以及 2 个配合物的固体和液体荧光性质。

关键词：水热合成；配位化学；晶体结构；荧光性质
中图分类号：O614.24+1 **文献标识码**：A **文章编号**：1001-4861(2018)03-0545-06
DOI:10.11862/CJIC.2018.060

Two Mono- and Binuclear Zn(Ⅱ) Coordination Complexes Containing 4-Pyridyl-*NH*-1,2,3-triazole Ligand: Syntheses, Structures and Photoluminescence Properties

LEI Xue CHEN Yun-Zhou LI Yuan-Xiang JIA Li-Hui* CHEN Yun-Feng*
(*School of Chemistry and Environmental Engineering, Wuhan Institute of Technology, Wuhan* 430073, *China*)

Abstract: Two Zn(Ⅱ) coordination complexes, $[Zn_2(L)_2Cl_4]$ (**1**) and $[Zn(L)_2Cl_2] \cdot 2H_2O$ (**2**) (L=4-pyridiyl-*NH*-1,2,3-triazole) are synthesized by reaction of $ZnCl_2 \cdot 2H_2O$ with rigid ligand L. Single crystal diffraction reveals that **1** and **2** crystallizes in space groups, $P\bar{1}$ and $P2_1/n$, respectively. In the structures of **1** and **2**, supramolecular interactions play important role in forming 3D structures. Photoluminescent properties of **1** and **2** in solid state and dilute methanolic solutions have been investigated in detail. CCDC: 1554502, **1**; 1554503, **2**.

Keywords: hydrothermal synthesis; coordination chemistry; crystal structure; photoluminescence properties

0 Introduction

Coordination polymers (CPs), known as a type of organic-inorganic hybrid materials, are very promising for developing multifunctional luminescent materials[1-3]. Both the inorganic and the organic moieties can provide the platforms to generate luminescence, while metal-ligand charge transfer also contributed to luminescence[4]. The size and nature of metal ions, the orientation and arrangement of ligands, even the supramolecular interactions can affect the fluorescent properties of CPs[5-8]. Therefore, controlling these interactions by exploring various metals and organic ligands is crucial for tuning the luminescence properties for a particular application.

In the recent years, a great deal of attention has

收稿日期:2017-09-18。收修改稿日期:2017-11-22。
国家自然基金(No.21002076,21441007)、湖北省教育厅重点项目(No.D20131506)和武汉工程大学研究生创新基金(No.CX2016167)资助。
*通信联系人。E-mail:jialihui715@wit.edu.cn,yfchen@wit.edu.cn

been devoted to the synthesis of N-heterocyclic-based coordination polymers due to their surprising structural variability[9-12]. With the development of the Cu(I) catalyzed azide-alkyne cycloaddition (CuAAC) reaction[13-14], 1,2,3-triazole which could exhibit abundant coordination modes has been appreciated as a metal coordination ligand[15-19]. Since the extended π-systems of small florescence molecules facilitate the ligand-centered $\pi\rightarrow\pi^*$ transition[20-23], we have intended to add aromatic groups to 1,2,3-triazole and incorporate this moiety into coordination polymers. Based on our previous work about the syntheses of 1,2,3-triazoles and related complexes[24-28], we chose the small molecular 4-pyridyl-*NH*-1,2,3-triazole as the ligand. On the other hand, zinc complexes have received much attention because they not only exhibit interesting structures but also show better luminescent properties[29-32]. Herein, we report the syntheses, structures, and luminescent properties of two coordination complexes $[Zn_2(L)_2Cl_4]$ (**1**) and $[Zn(L)_2Cl_2]\cdot 2H_2O$ (**2**).

1 Experimental

1.1 Material and measurements

All reagents were purchased and used without further purification. Thermogravimetric analysis (TGA) was performed on a NETZSCH TG 209 F3 thermogravimetric analyzer in flowing N_2 (20 mL·min^{-1}) with a heating rate of 10 ℃·min^{-1}. The FT-IR spectra were recorded from KBr pellets in the range of 4000~450 cm^{-1} on an Agilent FT-IR spectrometer. The luminescence spectra for powdered samples and aqueous samples were recorded on Perkin Elmer Florescence Spectrometer LS S5 with a xenon arc lamp as the light source with the pass width of emission and excitation spectra of 15 and 2.5 nm. The UV-Vis spectra for samples (0.1 mmol·L^{-1} in methanol) were recorded on Perkin Elmer UV WinLab 6.0.4.0738/Lambda35 1.27. Elemental analysis of carbon, nitrogen, hydrogen was performed using an Elementar Vario MICRO CUBE (Germany) analyzer. PXRD data for complexes **1** and **2** were collected in the range of 5°~50° for 2θ on crystalline samples using a XPERT-PRO diffractometer with Cu *K*α radiation (λ=0.154 18 nm, 40 kV, 40 mA) in flat-plate geometry at room temperature. The experimental powder X-ray diffraction pattern was compared to the calculated one from the single-crystal structure to identify the phase of the sample (Fig.S6~S7).

1.2 Preparations of complexes 1 and 2

A mixture of $ZnCl_2\cdot 2H_2O$ (0.15 mmol), L (0.15 mmol) and acetonitrile (5 mL) was placed in a 20 mL glass bottle. The mixture was sealed and heated at 80 ℃ for 48 hours and cooled to room temperature naturally. Grey block crystals of **1** was obtained by filtration. IR (KBr, cm^{-1}): 3 112(s), 2 963(m), 1 609(m), 1 139(m), 711(w). Elemental analysis Calcd. for $C_{14}H_{12}Cl_4N_8Zn_2$(%): C 29.77, H 2.14, N 19.84; Found (%): C 29.61, H 2.04, N 19.65. To a solution of 25.8 mg $ZnCl_2\cdot 2H_2O$ (0.15 mmol) in 1 mL distilled water was added 22.1 mg L (0.15 mmol) in 4 mL acetonitrile. The mixture was left to evaporate in air until colorless block crystals of **2** were obtained after 3 days. IR (KBr, cm^{-1}): 3 342(s), 3 042(m), 2 732(m), 2 362(m), 1 615(m), 1 445(m), 1 337(w), 1 243(m), 787(s), 714(w) cm^{-1}. Elemental analysis Calcd. for $C_{14}H_{16}O_2Cl_2N_8Zn$ (%): C 36.19, H 3.47, N 24.12; Found(%): C 36.02, H 3.22, N 24.00.

1.3 Single-crystal X-ray crystallography

Single crystals of complexes **1** and **2** suitable for single-crystal X-ray diffraction were grown up from acetonitrile solution under hydrothermal reaction and slow evaporation at room temperature. The crystallographic data for the single crystals of **1** and **2** were collected on a CrysAlis PRO 1.171.39.7a (Rigaku OD, 2015) employing graphite-monochromated Mo *K*α radiation (λ=0.071 073 nm). Empirical absorption correction using spherical harmonics, implemented in SCALE3 ABSPACK scaling algorithm. All structures were solved by direct methods using the Olex2 program with the SHELXTL package and refined with SHELXL[33-34]. Hydrogen atoms were added geometrically and refined with riding model position parameters and fixed isotropic thermal parameters. Crystallographic data for **1** and **2** are listed in Table 1, selected bond lengths and angles, and hydrogen bond lengths and angles are listed in Table S1 and S2.

Table 1　Crystallographic data of 1 and 2

Complex	1	2
Empirical formula	$C_{14}H_{12}Cl_4N_8Zn_2$	$C_{14}H_{16}O_2Cl_2N_8Zn$
Formula weight	564.86	464.62
Crystal system	Triclinic	Monoclinic
Space group	$P\bar{1}$	$P2_1/n$
a / nm	0.750 9(1)	0.804 5(1)
b / nm	0.809 3(1)	0.770 3(1)
c / nm	0.886 9(1)	1.517 6(2)
α / (°)	88.708(9)	
β / (°)	73.294(9)	94.614(8)
γ / (°)	71.798(11)	
V / nm^3	0.489 0(1)	0.937 4(2)
Z	1	2
D_c / (g·cm^{-3})	1.918	1.646
μ / mm^{-1}	3.018	1.623
Crystal size / mm	0.2×0.1×0.1	0.3×0.3×0.1
θ range / (°)	2.7~26.0	2.7~25.0
Reflection collected	2 786	8 826
Independent reflection	1 919	1 648
Observed reflection [$I>2\sigma(I)$]	1 469	1 360
R_{int}	0.054 4	0.038 7
GOF on F^2	1.083	1.116
R_1, wR_2 [$I\geqslant 2\sigma(I)$]	0.046 2, 0.119 4	0.028 9, 0.069 2
R_1, wR_2 (all data)	0.054 7, 0.131 4	0.039 7, 0.073 8
Largest diff. peak and hole / (e·nm^{-3})	867 and −1 088	528 and −281

CCDC: 1554502, **1**; 1554503, **2**.

1.4　Density functional theory calculations

The initial structures of complex **1** and complex **2** were obtained from the single-crystal data and the initial structure of free ligand L was obtained from that of complex **2** by deleting other atoms. The geometry optimization were performed at B3LYP/6-31G(d,p)[35-37] theory level in methanol solvent with PCM model by using Gaussian 16 software[38]. At the optimized structures, harmonic vibrational frequencies (all real) were calculated to confirm that all optimized structures correspond to energy minima. Molecular orbitals cube files were generated and visualized with GaussView 6.0.16.

2　Results and discussion

2.1　Crystal structures

X-ray structural analyses reveal that the **1** and **2** crystallize in different space groups, $P\bar{1}$ and $P2_1/n$, respectively. In the structure of **1**, Zn^{2+} exhibits five coordination (the degree of trigonality, τ=0.43)[39] with one terminal Cl, two μ_2-Cl and two N atoms from a chelating L (Fig.1a). There are three kinds of H-bonds within the molecular units. One is the strong intermolecular H-bond, N4−H4⋯Cl1 (H4⋯Cl1 0.229 1(55) nm, N4−H4⋯Cl1 162.55(558)°), connecting the neighbor units to form dimer in *ac* plane. The second H-bond originates from C2−H2⋯Cl2, with $d_{C2\text{-}H2}$ = 0.278 2(60) nm and ∠C2−H2⋯Cl2=169.00(572)°. The third is an intramolecular H-bonds, C7−H7⋯Cl1 (H7⋯Cl1 0.273 5(48) nm, C7−H7⋯Cl1 160.98(370)°) (Fig.S1). Besides the H-bonds, there is one offset π-π stacking interaction between two pyridine (C_5N) rings with a centroid-to-centroid distance of 0.362 0(1) nm and an interplane separation of 0.333 4(1) nm (Fig. 1b). These intermolecular interactions are important

for the crystallization of **1**. The Zn1 ⋯ Zn1^{i} distance is 0.357 2(1) nm and the Zn1-Cl2-Zn1^{i} angle is 93.880(39)°[40-41].

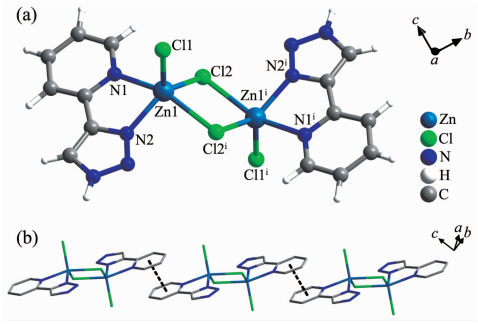

Dotted line represents the interaction between two pyridine rings; Symmetry codes: ^{i} $-x+1, -y, -z+1$

Fig.1 Structure of **1**: (a) Coordination environment of Zn(Ⅱ); (b) π-π interactions

In the structure of **2**, Zn^{2+} exhibits six coordinated with two terminal Cl, four N atoms from chelating L (Fig.2a). Four intermolecular H-bonds were found. The first is C4–H4⋯Cl1, with $d_{H4\cdots Cl1}$=0.281 6(33) nm and ∠C4–H4⋯Cl1=159.07(260)°. As a result, the adjacent mono-zinc(Ⅱ) blocks are assembled into H-bonded one dimensional chains along *a* direction with the shortest intrachain separation of 0.804 5(1) nm (Fig.S2a). As for the *bc* plane, three kinds of intermolecular H-bonds connect the chains. Each H_2O acts as a double H-bond donor leading to intermole-cular O1W–H1WA⋯Cl1 (H⋯Cl 0.232 2(39) nm, O–H⋯Cl 170.33(363)°) and O1W–H1WB⋯Cl1 (H⋯Cl 0.254 0(32) nm, O–H⋯Cl 164.82(33)°). Moreover, the water molecular serve as an H-bond acceptor, which generate strong hydrogen bonding N4–H4A⋯O1W, with $d_{H4A\cdots O1W}$=0.189 7(31) nm and ∠N4–H4A⋯O1W=174.90(311)° (Fig.2b). The intramolecular H-bond is C1–H1⋯N3 ($d_{H1\cdots N3}$= 0.263 7(24) nm, ∠C1–H1⋯N3=149.28(195)°) (Fig. S2b).

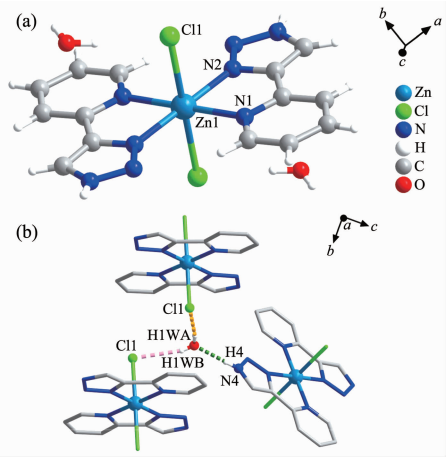

Fig.2 Structure of **2**: (a) Coordination environment of Zn(Ⅱ); (b) Various hydrogen bonds generated by H_2O

2.2 Fluorescent properties

The phase purities of **1** and **2** have been confirmed by PXRD (Fig.S6 and S7). Firstly, the photoluminescence spectra of the free ligand L and the two Zn(Ⅱ) coordination complexes were measured in methanol (10 μmol·L^{-1}, λ_{ex}=301 nm). The free ligand L and the corresponding Zn coordination complexes exhibit similar emission spectra centered at λ_{em}=361 nm (Fig. 3). Compared with free L and Zn^{2+} ion, the enhancement of fluorescence intensity came up in the complexes **1** and **2**, and the mononuclear **2** is stronger than the dimer **1**. It is probably due to the coordination of L to the Zn(Ⅱ) center, increasing the conformational rigidity of the ligand, thereby reducing the nonradiative decay of the intraligand (π-π*) excited state[42].

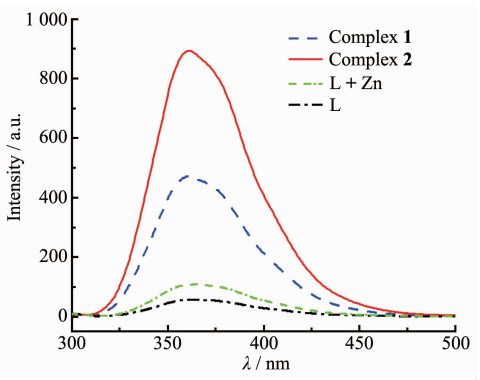

λ_{ex}=301 nm, c=10 μmol·L^{-1}

Fig.3 Emission spectra of the complexes and the ligand recorded at room temperature in methanol

Further, the solid-state photoluminescent properties of Zn(Ⅱ) coordination complexes **1** and **2** have been investigated together with free ligand L at room temperature (Fig.4). Ligand L displays strong green photoluminescence with a maximum emission peak at 517 nm upon excitation at 260 nm, which could probably be attributed to the π*-π and π*-*n*

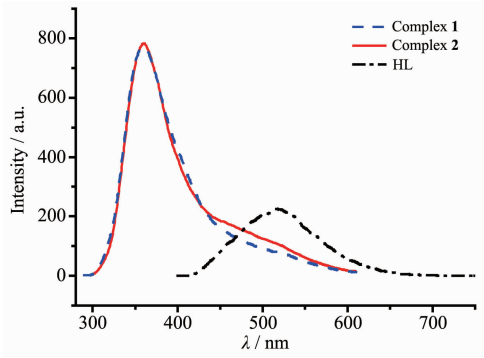

λ_{ex}=260 nm

Fig.4　Room-temperature solid-state emission spectra for L, **1** and **2**

transitions[43-45]. For the complexes **1** and **2**, excitation of the microcrystalline samples leads to the generation of strong blue fluorescent emissions with the same maximal peak occurring at 358 nm (λ_{ex}=260 nm). Obviously, this characteristic emission can probably be attributed to the intraligand charge transitions. As for the correlation of structure and fluorescent properties, the π-π packing in the L ligand and its coordination complexes have influence on the fluorescent properties[46]. From the photoluminescence spectra of the free ligand L (Fig.S8), the big change was observed in the methanol solution and solid state at room temperature, which is due to the enhancement of π-π packing in ligand under the condition of solid state. The observed blue-shift of the emission bands between the L ligand and the corresponding complexes **1**~**2** might tentatively originate from the weakened structure packing of ligand L because of the coordination with the metal ions.

2.3　Molecular orbitals

It can be concluded reasonably that the HOMO of ligand is π bonding orbital, and the HOMO of complex **2** is mainly based on coordinated chloride ions, while the HOMO of complex **1** is based on both coordinated chloride ions and the π-bonding orbitals of ligand. In contrast, the LUMOs of ligand and complexes **1** and **2** are mainly contributed by the π-antibonding orbits of ligand (Fig.5). As a consequence, the UV-Vis and luminescence spectra of complex **1** and **2** should be mainly assigned to charge transfer between chloride ions and ligand in nature[47].

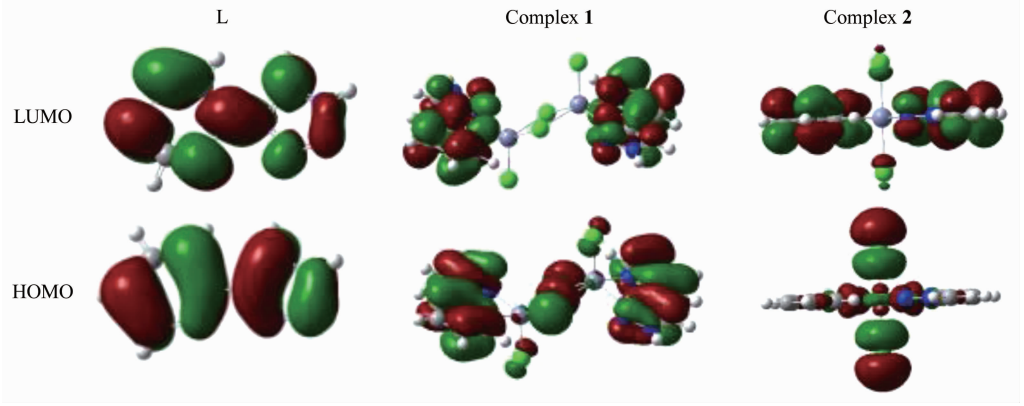

Fig.5　Frontier molecular orbits of complexes **1** and **2** from HOMO to LUMO

3　Conclusions

In summary, two new pyridyl triazole complexes of Zn (Ⅱ) were synthesized and their photophysical properties were explored. Structurally, the free ligand L coordinated with Zn(Ⅱ) in different ways, resulting in the mono- and di-nuclear Zn^{2+} complexes. With Cl^- occupying the axial positions, the complexes exhibit weaker π-π stacking compared with small-molecular ligand, which led to blue shift of the ligand in solid state.

Acknowledgements: The authors are grateful to Prof. ZHANG Yue-Xing and Prof. LIU Jun-Liang on density functional theory calculations.

Supporting information is available at http://www.wjhxxb.cn

References:

[1] Suh M P, Cheon Y E, Lee E Y. *Chem. Rev.*, **2008**,**252**:1007

-1026

[2] Maspoch D, Ruiz-Molina D, Veciana J. *Chem. Soc. Rev.*, **2007**,**36**:770-818

[3] Rocha J, Carlos L D, Paz F A A, et al. *Chem. Soc. Rev.*, **2011**,**40**:926-940

[4] Cui Y J, Yue Y F, Qian G D, et al. *Chem. Rev.*, **2012**,**112**:1126-1162

[5] Xiang J, Li Z G, Zou H. *Cryst. Res. Technol.*, **2013**,**48**:87-93

[6] Yu F, Chu W K, Shen C, et al. *Eur. J. Inorg. Chem.*, **2016**, **24**:3892-3899

[7] XU Hai-Bing(徐海兵), CHEN Zhong-Ning(陈忠宁). *Chinese J. Inorg. Chem.*(无机化学学报), **2011**,**10**:1887-1903

[8] Huang Y Q, Wan Y, Chen H Y, et al. *New J. Chem.*, **2016**, **40**:7587-7595

[9] Aromi G, Barrios L A, Roubeau O, et al. *Coord. Chem. Rev.*, **2011**,**255**:248-546

[10]YAN Juan-Zhi(闫娟枝), LU Li-Ping(卢丽萍). *Chinese J. Inorg. Chem.*(无机化学学报), **2017**,**33**:1697-1704

[11]XIAO Bo-An(肖伯安), CHEN Shui-Sheng(陈水生). *Chinese J. Inorg. Chem.*(无机化学学报), **2017**,**33**:347-353

[12]Huang Y Q, Cheng H D, Chen H Y, et al. *CrystEngComm*, **2015**,**17**:5690-5701

[13]Rostovtsev V V, Green L G, Fokin V V, et al. *Angew. Chem., Int. Ed.*, **2002**,**41**:2596-2599

[14]Torne C W, Christensen C, Meldal M. *J. Org. Chem.*, **2002**, **67**:3057-3064

[15]Obata M, Kitamura A, Mori A, et al. *Dalton Trans.*, **2008**, **25**:3292-3300

[16]Uppal B S, Booth R K, Ali N, et al. *Dalton Trans.*, **2011**,**40**:7610-7616

[17]Connell T U, White J M, Smith T A, et al. *Inorg. Chem.*, **2016**,**55**:2776-2790

[18]Bai S, Jiang L, Zuo J L, et al. *Aust. J. Chem.*, **2013**,**66**:1029-1033

[19]Zou J Y, Gao H L, Shi W, et al. *CrystEngComm*, **2013**,**15**:2682-2687

[20]Xiang J, Lo L T, Leung C, et al. *Organometallics*, **2012**,**31**:7101-7108

[21]Ballardini R, Varani G, Indelli M T, et al. *Inorg. Chem.*, **1986**,**34**:3858-3865

[22]Donges D, Nagle J K, Yersin H. *Inorg. Chem.*, **1997**,**36**:3040-3048

[23]Outlaw V K, Zhou J, Bragg A, et al. *RSC Adv.*, **2016**,**6**:61249-61253

[24]Deng X C, Lei X, Nie G, et al. *J. Org. Chem.*, **2017**,**82**:6163-6171

[25]Chen Y F, Nie G, Zhang Q, et al. *Org. Lett.*, **2015**,**17**:1118-1121

[26]Hu Q Q, Liu Y, Deng X C, et al. *Adv. Synth. Catal.*, **2016**, **358**:1689-1693

[27]Ma C L, Wu J, Chen Y F. *Russ. J. Coord. Chem.*, **2015**,**41**:447-450

[28]Chen Y F, Wu J, Ma S, et al. *J. Mol. Struct.*, **2015**,**1089**:1-8

[29]Yuan G, Shao K Z, Du D Y, et al. *Solid State Sci.*, **2011**,**13**:1083-1091

[30]Du J Y. *Transition Met. Chem.*, **2004**,*29*:699-702

[31]Qin J S, Du D Y, Li M, et al. *J. Am. Chem. Soc.*, **2016**,**138**:5299-5307

[32]Zeng M H, Yin Z, Liu Z H, et al. *Angew. Chem. Int. Ed.*, **2016**,**55**:11407-11411

[33]Dolomanov O V, Bourhis L J, Gildea R J, et al. *J. Appl. Cryst.*, **2009**,**42**:339-341

[34]Sheldrick G M. *Acta Crystallogr., Sect. A*: *Found. Crystallogr.*, **2008**,**A64**:112-122

[35]Fernandez-Hernandez J M, Yang C H, Beltran J I, et al. *J. Am. Chem. Soc.*, **2011**,**133**:10543-10558

[36]Zhong A, Zhang Y X, Bian Y Z. *J. Mol. Graphics Modell.*, **2010**,**29**:470-480

[37]Zhang Y X, Cai X, Yao P, et al. *Chem. Eur. J.*, **2007**,**13**:9503-9514

[38]Frisch M J, Trucks G W, Schlegel H B, et al. *Gaussian* 16 *Software*, Gaussian Inc., Wallingford CT, **2016**.

[39]Addison A W, Rao T N, Reedijk J, et al. *J. Chem. Soc. Dalton Trans.*, **1984**:1349-1356

[40]Janiak C. *J. Chem. Soc. Dalton Trans.*, **2000**:3885-3896

[41]Jeffrey G A. *Crystallogr. Rev.*, **2003**,**9**:135-176

[42]Li Y W, Ma H, Chen Y Q, et al. *Growth Des.*, **2012**,**12**:189-196

[43]Xu C Y, Guo Q Q, Wang X J, et al. *Cryst. Growth Des.*, **2011**,**11**:1869-1879

[44]Hua J A, Zhao Y, Liu Q, et al. *CrystEngComm*, **2014**,**16**:7536-7546

[45]Meng F D, Zhang M D, Shen K, et al. *Dalton. Trans.*, **2015**, **44**:1412-1419

[46]Zhu X F, Yang Y, Jiang N, et al. *Z. Anorg. Allg. Chem.*, **2015**,**641**:699-703

[47]Scaltrito D V, Thompson D W, O′Callaghan J A, et al. *Coord. Chem. Rev.*, **2000**,**208**:243-266